ADVANCED FUNCTIONAL MATERIALS
www.afm-journal.de

Optically Transparent Antibacterial Films Capable of Healing Multiple Scratches

*Xu Wang, Yan Wang, Shuai Bi, Yongguo Wang, Xigao Chen, Lingying Qiu, and Junqi Sun**

Optically transparent antibacterial films capable of healing scratches and restoring transparency are fabricated by exponential layer-by-layer assembly of branched polyethylenimine (bPEI)/poly(acrylic acid) (PAA) films and post-diffusion of cetyltrimethylammonium bromide micelles encapsulated with antibacterial agent triclosan. The triclosan-loaded bPEI/PAA transparent films can effectively inhibit the growth of gram-positive and gram-negative bacteria by the sustained release of triclosan molecules. Healing of multiple scratches on the triclosan-loaded bPEI/PAA films can be conveniently achieved by immersing the films in water or spraying water on the damaged films, which also fully restores their transparency. The self-healing ability of these transparent antibacterial films originates from the ability of bPEI and PAA to flow and recombine in the presence of water. The triclosan-loaded bPEI/PAA films have satisfactory mechanical stability under ambient conditions, and thus show potential for application as transparent protective films with antibacterial properties.

1. Introduction

Transparent films are useful in various optical and display devices and as protective materials.[1] Two issues usually arise for transparent films that are in direct contact with people. On the one hand, accidental scratches on the transparent films during usage over time can lead to light scattering and blur of displayed pictures or words underlying the films. On the other hand, frequent contact with fingers can leave behind infectious bacteria and viruses on the surface of transparent films, which are then readily transferred to people who touch them.[2] It is well known that 80% of infectious diseases are transferred by direct and indirect touch.[3] Bacteria and viruses on touch screens can pose a severe threat to human health, especially on touch screens for public usage. Considering these facts, it is highly desirable to fabricate transparent films that are antibacterial and capable of healing scratches for application in optical and display devices.

Self-healing materials[4] can repair damage by using the resources inherently available to the materials in either an autonomic[5] or nonautonomic[6] way, depending on whether or not external assistance such as heat, light, or humidity is required.[6] The self-healing ability of artificial materials can extend their service lives, facilitate their maintenance and increase their reliability. Current research interests regarding self-healing materials are gradually moving from restoring mechanical and structural properties to healing of functions.[7] A self-healing function has been successfully integrated into anticorrosive,[8] superhydrophobic,[9] superoleophobic[10] and electrically conductive materials.[11] Despite their practical applications, the fabrication of transparent self-healing films is challenging.[4b] Microcapsules are frequently used as carriers to incorporate healing agents in extrinsic self-healing materials, where rupture of the embedded capsules initiates the healing process.[5a,12] The fabrication of transparent self-healing materials or films by the capsule method is technically difficult because microsized capsules strongly scatter visible light.[13] Several factors must be optimized to use microcapsules in transparent self-healing materials: the refractive indices of the capsules and embedded healing agents must be close to that of the matrix, the size of the capsules should be as small as possible to avoid visible light scattering, and the concentration of capsules in the matrix must be low to avoid their aggregation. Unfortunately, these requirements are difficult to simultaneously satisfy in one film, because the decrease of both capsule size and concentration reduces the quantity of healing agent available to repair the damaged region, and therefore decreases healing ability. Recently, Jackson et al. fabricated transparent self-healing polymethylmethacrylate (PMMA) films by dispersing microcapsules containing refractive index-matching dibutyl phthalate plasticizer in PMMA.[14] When small capsules (1.5 μm in diameter) with a low loading concentration are used, transparent PMMA films capable of partially healing cracks are obtained. PMMA films capable of fully healing cracks are obtained by using large capsules (75 μm in diameter), which comes at the expense of increased light scattering. Different from extrinsic self-healing materials that require inclusion of specific healing agents, intrinsic ones self-repair through the inherent reversibility of chemical bonds or physical interactions, such as reversible covalent and non-covalent bonds.[6a,b] Intrinsic self-healing is promising for fabricating materials or films that are transparent in the visible region because no additional healing agent is required; this

Dr. X. Wang, Y. Wang, S. Bi, Dr. Y. Wang, X. Chen, L. Qiu, Prof. J. Sun
State Key Laboratory of Supramolecular Structure and Materials, College of Chemistry
Jilin University
Changchun, 130012, PR China
E-mail: sun_junqi@jlu.edu.cn

DOI: 10.1002/adfm.201302109

avoids the intractable problems of optimization of capsule size and matching the refractive indices of the matrix, capsule and healing agent. Moreover, multiple healings of transparency in a given location is expected to be realized because the extinction of healing agent does not exist. In recent years, transparent bulk self-healing materials such as chemical gels and supramolecular rubbers that use reversible covalent and noncovalent bonds to heal based on the intrinsic self-healing method have been fabricated.[15] However, there are few reports of self-healing films capable of restoring transparency after damage,[16] and no optically transparent antibacterial films capable of healing scratches have been developed.

The layer-by-layer (LbL) assembly technique, which involves alternate deposition of species with complementary noncovalent interactions, is an inexpensive yet versatile way to fabricate conformal films on virtually any substrate.[17] Because all species are deposited in a predesigned LbL fashion, LbL assembly enables precise control over the chemical composition and structure of films on both micro- and nanoscales. LbL-assembled films have multiple applications in solar energy conversion,[18] separation,[19] optical[20] and electrical devices[21] and as smart materials capable of responding rapidly to various stimuli.[22] Recently, LbL assembly has been used to fabricate self-healing films.[6c,9a,11a] Taking advantage of exponential LbL assembly to rapidly fabricate micrometer-thick polyelectrolyte multilayer films and control polyelectrolyte interpenetration, we successfully produced intrinsic self-healing polyelectrolyte films capable of healing micrometer-sized defects.[16] These exponentially-grown LbL-assembled branched polyethylenimine (bPEI)/poly(acrylic acid) (PAA) films can autonomically repair cuts several tens of micrometers deep and wide when water is sprayed on them. Unfortunately, these bPEI/PAA self-healing films have an extremely rough surface, which leads to strong visible light scattering. Here we present the first example of colorless, optically transparent antibacterial films capable of healing damage caused by mechanical abrasion. These transparent self-healing films can also prohibit the growth of both gram-negative and gram-positive bacteria, *Escherichia coli* (*E. coli*) and *Bacillus subtilis* (*B. subtilis*), respectively, by the sustained release of triclosan from the films. Scratches on the films caused by mechanical abrasion can be completely repaired by immersing the films in water or spraying water on them, and their original transparency is fully restored. Importantly, the healing process can be repeated multiple times for different damage events in a given region. The optically transparent self-healing films with antibacterial ability have hardness comparable to a commercially available screen protector film, so they show promise for application as protective films with reliable antibacterial properties to extend the lifespan of optical and electrical devices.

2. Results and Discussion

2.1. Fabrication of Transparent Polyelectrolyte Films

Polycation bPEI and polyanion PAA were alternately assembled to fabricate transparent (bPEI/PAA)*n (where n represents the number of film deposition cycles, a half cycle means that bPEI is the outmost layer) films where electrostatic interaction and hydrogen bonding between amine and carboxylic acid groups was the main driving force for film fabrication. The chemical structures of bPEI and PAA are shown in the inset of **Figure 1**. Compared with the previously fabricated bPEI/PAA films with rough surfaces,[16] three parameters were optimized to achieve bPEI/PAA films with smooth surfaces: (i) PAA with a lower molecular weight than that used previously (M_w ca. 100 000) was employed; (ii) The concentration of bPEI and PAA dipping solutions was decreased from 4 mg mL^{-1} to 2 mg mL^{-1}, and the pH of bPEI and PAA aqueous solutions was 10.5 and 3.0, respectively; (iii) bPEI rather than PAA was set as the outmost layer of the bPEI/PAA films. Compared with linear PAA, bPEI with a branched structure is more flexible and has better ability to cover defects in the bPEI/PAA films. As a result, the surface of bPEI/PAA films with bPEI as the outmost layer is smoother than that with PAA as the outmost layer. The thicknesses of the (bPEI/PAA)*n films were determined from their corresponding cross-sectional scanning electron microscopy (SEM) images. As shown in Figure 1a, the (bPEI/PAA)*n films exhibit typical exponential deposition behavior for the initial 15 deposition cycles, and thereafter rapid linear deposition behavior with an increment of ~1.2 μm per deposition cycle. The rapid exponential LbL growth of the bPEI/PAA films is ascribed to the "in-and-out" diffusion of bPEI and PAA during film fabrication.[16,23] A (bPEI/PAA)*30.5 film, which has a constant thickness of 17.8 ± 0.5 μm, is optically transparent with a transmittance of ~85% in the visible region (curve a in **Figure 2**).

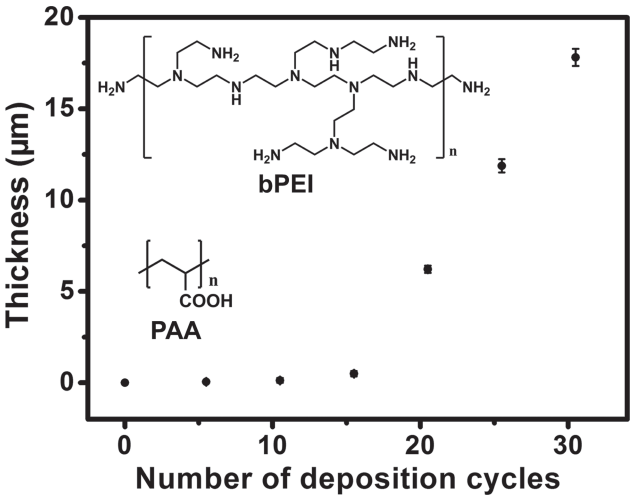

Figure 1. Thickness of bPEI/PAA films as a function of the number of deposition cycles. Inset shows the chemical structures of bPEI and PAA.

2.2. Loading and Release of Triclosan within Transparent Polyelectrolyte Films

Triclosan (5-chloro-2-(2,4-dichlorophenoxy)-phenol) is a broad-spectrum antimicrobial agent that is widely used in personal care products and kitchen utensils. Hydrophobic triclosan molecules (inset of **Figure 3**b) are difficult to incorporate directly into LbL-assembled films. Hammond and co-workers first encapsulated triclosan into polymeric micelles, and then

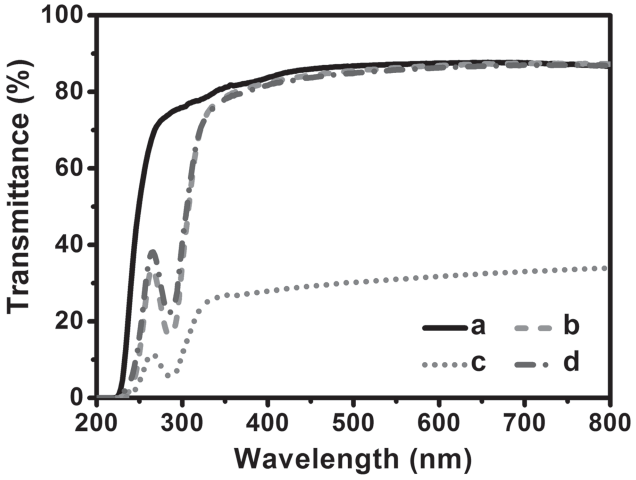

Figure 2. UV-vis transmission spectra of a (bPEI-PAA)*30.5 film (curve a), triclosan-(bPEI-PAA)*30.5 film (curve b), triclosan-(bPEI-PAA)*30.5 film after scratching (curve c) and self-healed triclosan-(bPEI-PAA)*30.5 film (curve d).

LbL-assembled the micelles with a partner polyelectrolyte to produce various antibacterial films.[24] To retain the self-healing ability of the bPEI/PAA films, we first encapsulated triclosan into cetyltrimethylammonium bromide (CTAB) surfactant micelles. The triclosan-loaded CTAB micelles (denoted triclosan@CTAB) were then loaded into the bPEI/PAA films by immersing the films in aqueous triclosan@CTAB solution. For simplicity, the triclosan-loaded (bPEI/PAA)*n films are abbreviated as triclosan-(bPEI/PAA)*n. The loading process of triclosan in (bPEI/PAA)*30.5 films deposited on quartz substrates was monitored by UV-vis absorption spectroscopy. As shown in Figure 3a, the characteristic absorbance of triclosan at 281 nm increases with immersion time. Rapid loading of triclosan in the (bPEI/PAA)*30.5 film was achieved within 30 min, after which the loading rate slowed (inset of Figure 3a). Here, (bPEI/PAA)*30.5 films were immersed in aqueous triclosan solution for 2 h, which generated films with a loading capacity for triclosan of 6.1 ± 0.7 μg cm^{-2}. The time-dependent release of triclosan from the (bPEI/PAA)*30.5 films at room temperature is shown in Figure 3b. The triclosan-(bPEI/PAA)*30.5 film releases triclosan relatively quickly in the initial 12 h because the release kinetics are diffusion-controlled.[25] Then, sustained release of triclosan in water capable of lasting for an extremely long time of over 20 days was observed. The release of triclosan from the bPEI/PAA films is caused by the disintegration of the incorporated CTAB micelles in water because CTAB was detected in the releasing solution by Fourier transform infrared spectroscopy. The target bPEI/PAA films are generally used in air under ambient conditions of mild humidity rather than in water. The hydrophilic bPEI/PAA films can absorb water from the surrounding environment, which expels the hydrophobic triclosan from the water-rich film to the film surface to inhibit bacterial growth (see the Supporting Information). The humidity-triggered release of hydrophobic molecules from hydrophilic polyelectrolyte films has been successfully used to fabricate self-healing superhydrophobic coatings.[9a] The release of triclosan from the bPEI/PAA films in air with a mild humidity can last

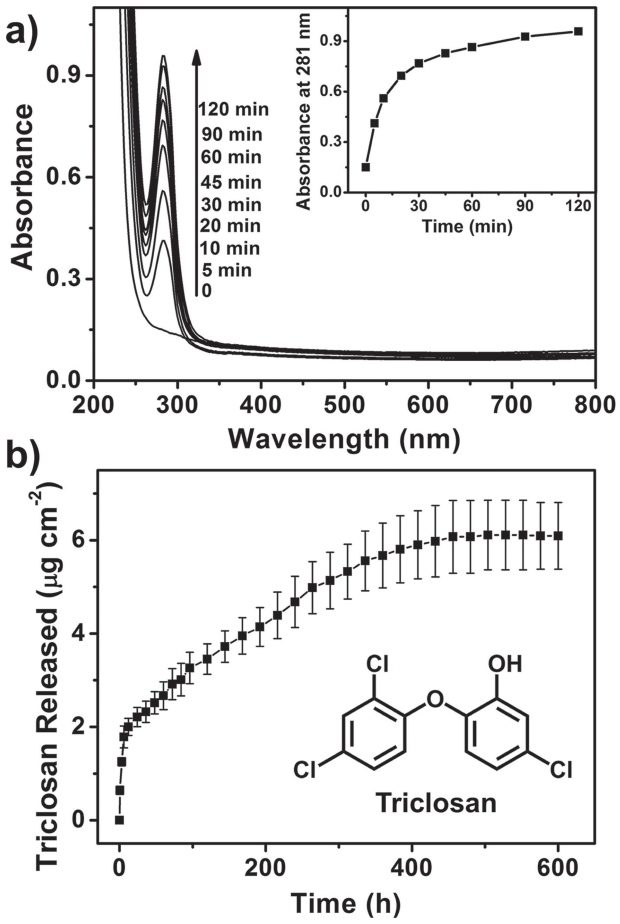

Figure 3. (a) UV-vis absorption spectra of a triclosan-(bPEI/PAA)*30.5 film with different loading times. (b) Time-dependent release profile of triclosan molecules from a triclosan-(bPEI/PAA)*30.5 film in water. Inset in (a) is a time-dependent loading profile of triclosan molecules in a (bPEI/PAA)*30.5 film. The chemical structure of triclosan is shown in the inset in (b).

for an even longer time than in water, which means they can maintain their antibacterial properties during extended use.

2.3. Antibacterial Ability of Triclosan-Loaded bPEI/PAA Films

E. coli and *B. subtilis* were selected as model gram-negative and gram-positive bacteria, respectively. The antibacterial properties of triclosan-(bPEI/PAA)*30.5 films was investigated using a modified Kirby-Bauer method.[26] Silicon substrates coated with triclosan-(bPEI/PAA)*30.5 films were gently placed on cultures of *E. coli* and *B. subtilis* in a Luria Bertani (LB) agar plate. As shown in **Figure 4**, after 24 h of incubation, the triclosan-(bPEI/PAA)*30.5 films caused a clearly visible zone of inhibition (ZOI) for both *E. coli* and *B. subtilis*, indicating that the released triclosan retains its activity and is effective at prohibiting the growth of both gram-negative and gram-positive bacteria. Films without triclosan did not exhibit antibacterial ability. Triclosan prohibits the growth of bacteria by binding to bacterial enoyl-acyl carrier protein reductase enzyme (ENR), which in

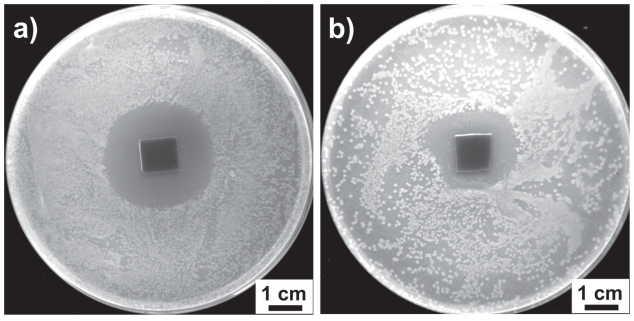

Figure 4. Agar plates of (a) *E. coli* and (b) *B. subtilis* growth inhibited by release of triclosan from triclosan-loaded (bPEI/PAA)*30.5 films.

turn prohibits synthesis of fatty acids necessary for reproducing and building cell membranes of bacteria.[27] Because humans do not have an ENR enzyme, triclosan is relatively non-toxic to humans. The humidity-triggered release of triclosan facilitates the application of the antibacterial triclosan-(bPEI/PAA)*30.5 films under an ambient environment with a mild humidity.

2.4. Multiple Healing Transparency of Antibacterial bPEI/PAA Films

The triclosan-(bPEI/PAA)*30.5 films were first scratched with 1500-grit sandpaper and then immersed in deionized water to examine their ability to self-heal scratches (**Figure 5**a). The healing process was monitored by visual observation, atomic force microscopy (AFM) and UV-vis transmission spectroscopy. The as-prepared triclosan-(bPEI/PAA)*30.5 films are optically transparent with a transmittance of ~85% in the visible region (Figure 5b and curve b of Figure 2). The AFM image in Figure 5e shows that the as-prepared triclosan-(bPEI/PAA)*30.5 films have a smooth surface. After being repeatedly scratched by sandpaper, obvious scratches appear on the films (Figure 5c). An AFM image reveals that the sandpaper formed grooves that were 4.3 ± 1.0 μm wide and 1.3 ± 0.4 μm deep on the films (Figure 5f). The scratched films become translucent with transmittance below 40% (curve c of Figure 2). The scratches on the damaged triclosan-(bPEI/PAA)*30.5 films can be conveniently repaired by immersing the films in water for 30 min, which also fully restores the original transparency of the films (Figure 5d and curve d of Figure 2). The surface of the self-healed triclosan-(bPEI/PAA)*30.5 films is smooth again (Figure 5g).

Full healing of the scratches on the transparent antibacterial triclosan-(bPEI/PAA)*30.5 films requires immersion in water for ~30 min. Alternatively, scratches on the films can be healed when water is sprayed on the damaged film (see the Supporting Information, Movie 1). The time-dependent self-healing process was monitored with an optical microscope, as shown in **Figure 6**. After damage by the sandpaper, dense scratches appeared in the optically smooth film (Figure 6a and b). The damaged film showed a strong tendency to heal scratches after being immersed in water for a short time of ~10 s (Figure 6c).

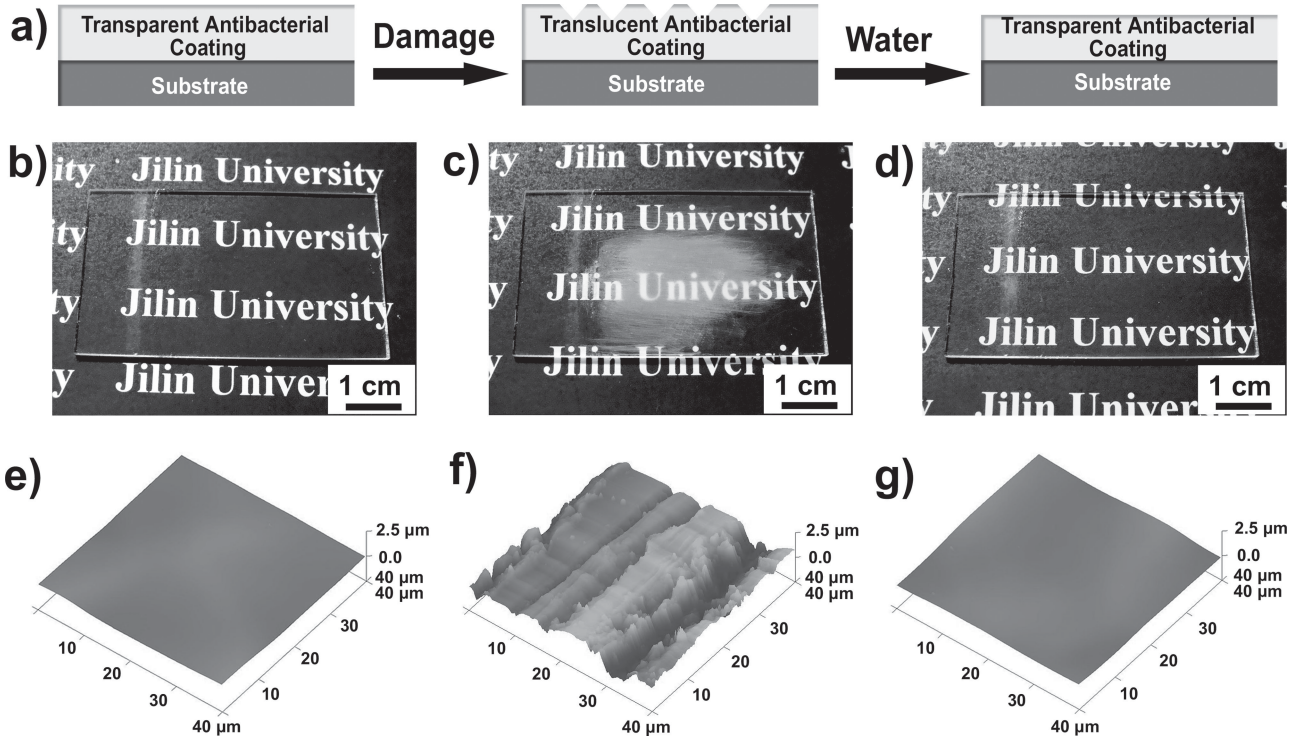

Figure 5. (a) Schematic illustration of the damage and healing process of a triclosan-loaded bPEI/PAA film. (b–d) Digital images of a triclosan-(bPEI/PAA)*30.5 film on a glass substrate. (b) As-prepared film; (c) Film in (b) after being scratched with sandpaper; (d) Film in (c) after healing in water. (e–g) AFM images of a triclosan-loaded (bPEI/PAA)*30.5 film on a silicon substrate. (e) As-prepared film; (f) Film in (e) after being scratched with sandpaper; (g) Film in (f) after healing in water.

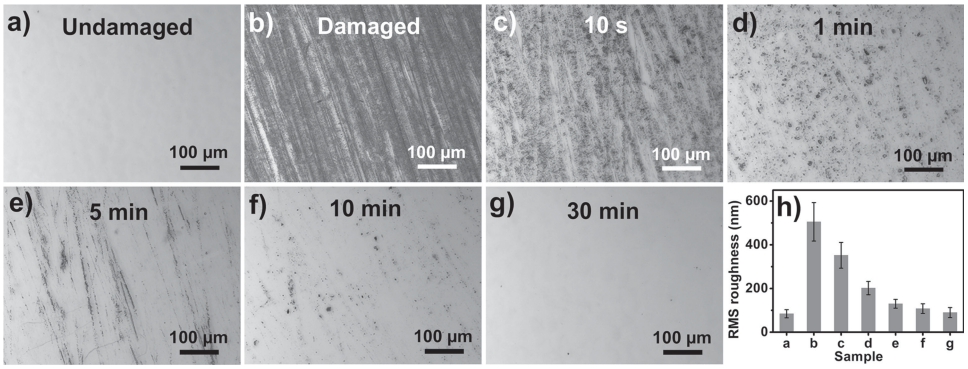

Figure 6. (a–g) Visual observation of the healing process of a triclosan-(bPEI/PAA)*30.5 film. (a) As-prepared film, (b) scratched film, (c–g) scratched film after immersion in water for (c) 10 s, (d) 1 min, (e) 5 min, (f) 10 min, and (g) 30 min. (h) The healing process of a triclosan-(bPEI/PAA)*30.5 film monitored by RMS roughness after immersion in water for different periods.

The scratches gradually disappeared with prolonged immersion in water (Figure 6d–g). All scratches were completely repaired after immersion in water for 30 min (Figure 6g). The healing process depicted in Figure 6b–g was further confirmed by the change of root-mean-square (RMS) roughness of the films characterized by AFM. As shown in Figure 6h, the as-prepared triclosan-(bPEI/PAA)*30.5 film has a RMS roughness of 84 ± 19 nm. The RMS roughness of the scratched film dramatically increased to 505 ± 88 nm, and then gradually decreased as the immersion time in water lengthened. The fully repaired film after immersion in water for 30 min has a RMS roughness of 90 ± 23 nm, which is similar to that of the original film, indicating complete healing.

The transparent antibacterial triclosan-(bPEI/PAA)*n films are a kind of intrinsic self-healing material, and can heal multiple times upon repeated damage events in a given location. The ability of the triclosan-(bPEI/PAA)*30.5 films to undergo transparency recovery multiple times was evaluated by monitoring their transmittance at 550 nm over five damage-healing cycles. As shown in **Figure 7**a, the as-prepared triclosan-(bPEI/PAA)*30.5 films had a transmittance of ~86% at 550 nm. After scratching with sandpaper, the films became translucent with their transmittance at 550 nm being in the range of 31% to 41%. The transmittance of the healed films at 550 nm after each healing process was higher than 85%. Meanwhile, the RMS roughness of the healed triclosan-(bPEI/PAA)*30.5 films was restored to the original value after five damage-healing cycles (Figure 7b). Because the transmittance of the films is strongly related to their roughness, restoration of their original RMS roughness further confirms that the triclosan-(bPEI/PAA)*30.5 films can undergo transparency recovery multiple times in a given location after repeated damage. The damage caused by scratching with sandpaper can lead to a large amount of polyelectrolyte loss from the film. As shown in **Figure 8**a, the as-prepared (bPEI/PAA)*30.5 films have a constant thickness of 17.8 ± 0.5 μm. The loading of triclosan@CTAB micelles increases film thickness by ~2.1 μm (Figure 8b). After five cycles of scratching/healing, the triclosan-(bPEI/PAA)*30.5 films are ~5.6 μm thinner because the polyelectrolytes in the undamaged areas move to repair the scratches (Figure 8c). This indicates that micrometer-thick films are needed to produce antibacterial, optically transparent bPEI/PAA films capable of healing damage multiple times in the same region. Moreover, thicker films can load more triclosan to maintain antibacterial ability for a long period.

The as-prepared bPEI/PAA films can repair scratches in the presence of water. The antibacterial triclosan-(bPEI/PAA)*30.5 films successfully inherited the self-healing ability of bPEI/PAA

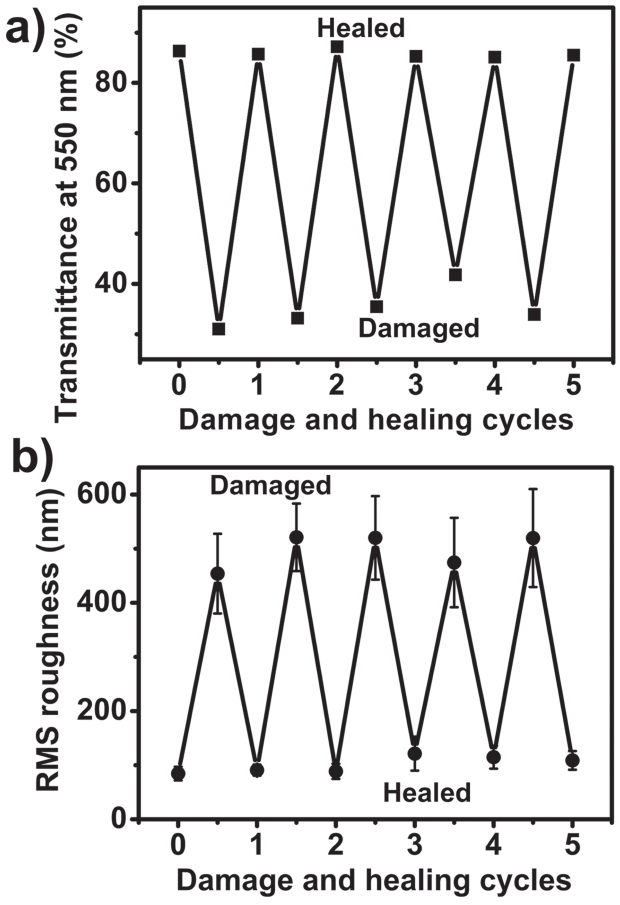

Figure 7. Changes of (a) transmittance at 550 nm, and (b) RMS roughness of a triclosan-(bPEI/PAA)*30.5 film during five damage-healing cycles.

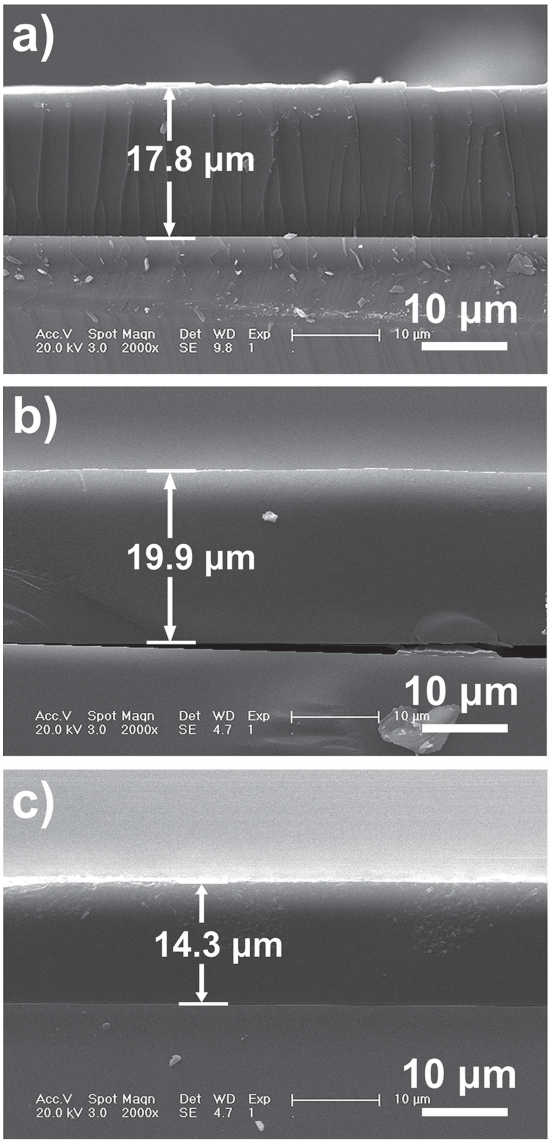

Figure 8. Cross-sectional SEM images of a (a) (bPEI/PAA)*30.5 film, (b) triclosan-(bPEI/PAA)*30.5 film, and (c) triclosan-(bPEI/PAA)*30.5 film after five damage-healing cycles.

films after the post-diffusion of triclosan@CTAB micelles. The post-diffusion of triclosan-loaded surfactant micelles provides at least two advantages in fabricating optically transparent antibacterial films: (i) The incorporated triclosan@CTAB micelles have minimal influence on the interdiffusion of polyelectrolytes in bPEI/PAA films, which is important for the self-healing ability of the resultant films; (ii) The release of triclosan occurs in pure water without additional triggers like specific pH or ionic strength. This allows the sustained release of triclosan in mildly humid environments, and means the antibacterial films will function under ambient conditions. It should be mentioned that self-healing procedure does not interfere with the antibacterial properties of the triclosan-(bPEI/PAA)*30.5 films. A triclosan-(bPEI/PAA)*30.5 film after 20 cycles of scratching with a sandpaper and healing in water exhibits clear antibacterial ability toward *E. coli* (see the Supporting Information).

2.5. Mechanical Properties of Transparent Antibacterial Films

The mechanical properties of the bPEI/PAA films before and after loading of triclosan under dry conditions and equilibrated in water were measured by nanoindentation.[1d,28] Indentations performed with the continuous stiffness measurement (CSM) technique give Young's modulus (E) and hardness (H) as a continuous function of indenter displacement. **Figure 9**a displays E of (bPEI/PAA)*30.5 films before and after loading of triclosan@CTAB micelles as a function of indentation depth. E for both films decreases rapidly with increasing indentation depth in the initial stage (<150 nm), followed by a plateau (~150 to 300 nm), and then a sharp rise (>300 nm). E in the plateau region is considered to be the "real" Young's modulus of the films, and is 9.2 ± 0.7 and 8.9 ± 1.2 GPa for (bPEI/PAA)*30.5 and triclosan-(bPEI/PAA)*30.5 films, respectively. The sharp increase in modulus at displacements over ~300 nm is consistent with the behavior of soft films on hard substrates.[29] H of the (bPEI/PAA)*30.5 and triclosan-(bPEI/PAA)*30.5 films as a function of indenter displacement is shown in Figure 9b. H is less sensitive to the substrate than E. H in the plateau region with penetration of 500–700 nm averaged at 0.43 ± 0.04 and 0.41 ± 0.05 GPa for (bPEI/PAA)*30.5 and triclosan-(bPEI/PAA)*30.5 films, respectively. The slight decrease of both E and H of the triclosan-(bPEI/PAA)*30.5 film compared with those of the (bPEI/PAA)*30.5 film implies that the incorporated triclosan@CTAB micelles slightly weaken the interactions between bPEI and PAA in the films. We also measured the mechanical properties of a commercially available screen protector film (RG Brand Screen Guard for Samsung I569/S5660, ~130 μm thick) under dry conditions by nanoindentation. E and H of this protector film were 4.6 ± 0.1 GPa and 0.41 ± 0.02 GPa, respectively (see the Supporting Information). Therefore, the mechanical properties of our self-healing, transparent antibacterial triclosan-(bPEI/PAA)*30.5 films under ambient conditions are comparable to those of a commercially available screen protector film designed for daily use.

Measurement of the mechanical properties of the films in water is critical to understand their healing mechanism. The NanoSuite test method "G-Series XP CSM Flat Punch Complex Modulus" using a flat-ended cylindrical punch with a diameter of 108.5 μm was used to measure the mechanical properties of the films in water. This method yields the storage and loss moduli of films as a function of frequency. The storage modulus (E') of the (bPEI/PAA)*30.5 films before and after triclosan loading is plotted as a function of frequency (Figure 9c), and increases with frequency. Because healing of the transparent antibacterial films occurs in static water, E' under a low frequency of 1 Hz were used to analyze the mechanical properties of the films in water. The (bPEI/PAA)*30.5 films before and after triclosan loading have E' of 110.3 ± 40.3 and 44.9 ± 11.6 MPa, respectively. The large decrease of E' of the films in water indicates that water acts as a plasticizer in the bPEI/PAA films. Water can partially break the electrostatic and hydrogen bonding interactions between bPEI and PAA, endowing the bPEI/PAA films with the ability to swell and flow in water. The migration of bPEI and PAA in (bPEI/PAA)*30.5 films is facilitated in water, promoting them to fill in the scratches on the film surface. The migrated bPEI and PAA then intermix in the

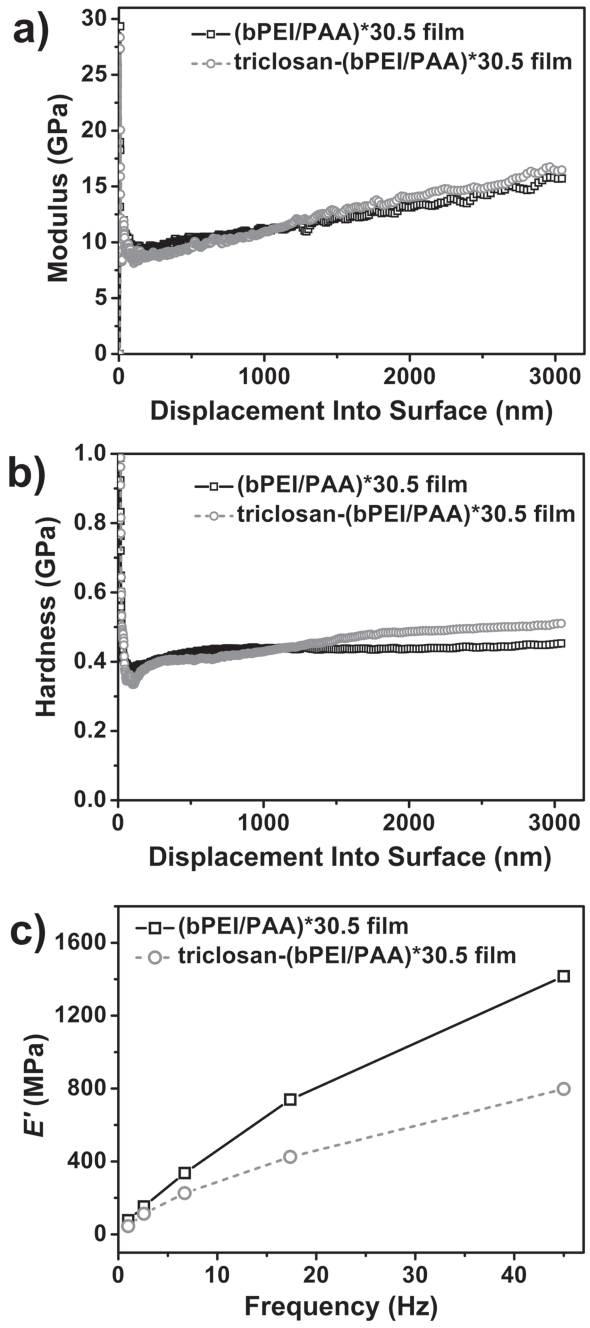

Figure 9. Mechanical properties of a (bPEI/PAA)*30.5 film before and after loading of triclosan@CTAB micelles determined by nanoindentation. Typical (a) Young's modulus (E), and (b) hardness (H) of a (bPEI/PAA)*30.5 film (□) and triclosan-(bPEI/PAA)*30.5 film (○) as a function of penetration depth. (c) Storage modulus (E') of a (bPEI/PAA)*30.5 film (□) and triclosan-(bPEI/PAA)*30.5 film (○) as a function of frequency.

scratched regions. Electrostatic and hydrogen bonding interactions between bPEI and PAA in the scratched regions reform as the films dry, which repairs the scratches and restores the optical transmission of the films. The incorporation of triclosan@CTAB micelles further decreases E' of the bPEI/PAA films, which increases the migration of bPEI and PAA, and therefore the ability of the film to heal scratches.

3. Conclusions

In the present study, we demonstrate that optically transparent, antibacterial films capable of restoring transparency can be fabricated by incorporating triclosan-loaded CTAB micelles into LbL-assembled bPEI/PAA films. The sustained release of triclosan from triclosan-(bPEI/PAA)*30.5 films endows the films with satisfactory antibacterial properties. Restoring the transparency of the films multiple times can be conveniently achieved by immersing the films in water or spraying water on the damaged films. The self-healing ability of the LbL-assembled bPEI/PAA films is not affected by the incorporation of triclosan-loaded CTAB surfactant micelles, which is ascribed to the high ability of bPEI and PAA to flow and recombine in water. The triclosan-(bPEI/PAA)*30.5 films have comparable mechanical robustness with a commercial screen protector film under ambient conditions, revealing their potential to act as clean, durable optical surfaces. LbL assembly allows film deposition on large, nonflat surfaces, further facilitating the applications of these optically transparent, antibacterial self-healing films. We believe that other kinds of functional species can be conveniently incorporated into LbL-assembled self-healing films by post-diffusion to fabricate a wide variety of self-healing films with novel functions. We are currently attempting to incorporate nanofillers into LbL-assembled films to fabricate self-healing, transparent robust films. The present study also demonstrates that intrinsic self-healing based on the reversibility of non-covalent bonds is a practical design to fabricate self-healing transparent films.

4. Experimental Section

Materials: bPEI (M_w ca. 750 000) and PAA (M_w ca. 100 000) were purchased from Sigma-Aldrich. Triclosan was purchased from Alfa Aesar. Analytical grade CTAB was purchased from Beijing Chemical Reagents Company. All chemicals were used without further purification. Deionized water was used for all experiments. The concentration of aqueous polyelectrolyte solutions used for film fabrication was 2 mg mL^{-1}, and pH was adjusted with either 1 M HCl or 1 M NaOH.

Film Preparation: Silicon, glass and quartz substrates were immersed in piranha solution (1:3 mixture of 30% H_2O_2 and 98% H_2SO_4) and heated until no bubbles were released. These cleaned substrates were suitable for LbL deposition of bPEI/PAA films without further modification. The substrate was first immersed in an aqueous bPEI solution (pH 10.5) for 15 min, followed by rinsing in four water baths for 1 min each. The substrate was then immersed in aqueous PAA solution (pH 3.0) for 15 min, followed by rinsing in four water baths for 1 min each. The bPEI/PAA multilayer films were prepared by repetition of the above deposition process in a cyclic fashion. No drying step was used in the deposition procedure unless it was in the last layer.

Loading and Release of Triclosan: CTAB micelle solution was obtained by dissolving CTAB (0.15 g) in deionized water (40 mL). A solution of triclosan in dichloromethane (200 µL, 80 mg mL^{-1}) was injected into the CTAB micelle solution, which was sonicated for ~1 h. After being left open overnight under continuous stirring to allow the dichloromethane to evaporate, the solution was filtered to remove any precipitated triclosan, giving triclosan@CTAB. Incorporation of triclosan@CTAB in (bPEI/PAA)*30.5 films was accomplished by immersing the films in triclosan@CTAB solution for ~2 h, followed by rinsing with water. To monitor the release of triclosan, a triclosan-(bPEI/PAA)*30.5 film deposited on a quartz slide was immersed in water (5 mL), which was replaced regularly to ensure constant release conditions. The amount of triclosan released from the film was determined using calibration curves for triclosan in water.

Film Characterization: UV-vis spectra were recorded on a Shimadzu UV-2550 spectrophotometer. SEM images were obtained on an XL30 ESEM FEG scanning electron microscope under vacuum. Films deposited on silicon wafers were cleaved, and their cross-sectional SEM images were recorded. All samples were coated with a thin layer of gold (2–3 nm) prior to SEM imaging. The digital images of films were captured under ambient conditions with a temperature of 25 °C and a relative humidity (RH) of 25% by a Sony Cyber-shot DSC-H10 camera in macro mode. Optical micrographs were taken with an Olympus BX-51 optical microscope. AFM images were taken on a commercial instrument, Veeco Company Nanoscope IV. AFM was performed in tapping mode using silicon cantilevers with a force constant of 40 N m^{-1}. The mechanical properties of the films were measured using an Agilent Nano Indenter G200 with the CSM method and XP-style actuator. All films, including the commercially available screen protector film, are deposited or attached on silicon wafers for measuring their mechanical properties. In the CSM method, the indenter is slowly pushed into the material while a small oscillation (~1 nm amplitude) is used to sense the instantaneous elastic stiffness of the contact. Elastic modulus and hardness are calculated from the measured quantities of force, indenter displacement, and contact stiffness (derived from the characteristics of the oscillation). A Berkovich diamond indenter with radius ≤20 nm was used to measure *E* and *H* of the films in air with ~18% RH at 30 °C by the "G-Series CSM Standard Hardness, Modulus and Tip Cal" test method. A flat-ended cylindrical punch made of diamond with a diameter of 108.5 μm was used to measure *E'* of the films in water by the "G-Series XP CSM Flat Punch Complex Modulus" method. Measurements were obtained at at least eight different sites for each film.

Bactericidal Activity of Films: *E. coli* and *B. subtilis* were selected as model gram-negative and gram-positive bacteria, respectively, to test the bactericidal activity of the triclosan-(bPEI/PAA)*30.5 films. *E. coli* and *B. subtilis* were incubated overnight at 37 °C in LB medium that contained tryptone (100 mg), yeast extract (50 mg) and NaCl (100 mg) in sterile distilled water (10 mL) at pH 7.0. Fresh cultures of both types of bacteria were diluted to a required concentration before each experiment. A modified Kirby-Bauer assay was conducted to determine the efficacy of the released triclosan to inhibit growth of bacteria. *E. coli* or *B. subtilis* suspension was coated on the surface of LB-agar plates (LB liquid media with 1.5% agar). Triclosan-(bPEI/PAA)*30.5 films on a silicon substrate (ca. 1 cm × 1 cm) were placed on the plates cultured with bacteria. The ZOI was observed after 24 h incubation at 37 °C. The test was carried out in triplicate to ensure reproducibility.

Supporting Information

Supporting Information is available from Wiley Online Library or from the author.

Acknowledgements

This work was supported by the National Natural Science Foundation of China (NSFC grants 21225419 and 21221063) and the National Basic Research Program (2013CB834503).

Received: June 21, 2013
Published online: August 13, 2013

[1] a) M. Vosgueritchian, D. J. Lipomi, Z. Bao, *Adv. Funct. Mater.* **2012**, *22*, 421; b) D. Yan, J. Lu, M. Wei, S. Qin, L. Chen, S. Zhang, D. G. Evans, X. Duan, *Adv. Funct. Mater.* **2011**, *21*, 2497; c) I. N. Kholmanov, M. D. Stoller, J. Edgeworth, W. H. Lee, H. Li, J. Lee, C. Barnhart, J. R. Potts, R. Piner, D. Akinwande, J. E. Barrick, R. S. Ruoff, *ACS Nano* **2012**, *6*, 5157; d) X. Liu, L. Zhou, F. Liu, M. Ji, W. Tang, M. Pang, J. Sun, *J. Mater. Chem.* **2010**, *20*, 7721.

[2] T. R. Julian, J. O. Leckie, A. B. Boehm, *J. Appl. Microbiol.* **2010**, *109*, 1868.

[3] P. M. Tierno, *The Secret Life of Germs: Observations and Lessons from a Microbe Hunter, Pocket Books*, New York, USA, **2001**.

[4] a) M. M. Caruso, D. A. Davis, Q. Shen, S. A. Odom, N. R. Sottos, S. R. White, J. S. Moore, *Chem. Rev.* **2009**, *109*, 5755; b) B. J. Blaiszik, S. L. B. Kramer, S. C. Olugebefola, J. S. Moore, N. R. Sottos, S. R. White, *Annu. Rev. Mater. Res.* **2010**, *40*, 179; c) R. P. Wool, *Soft Matter* **2008**, *4*, 400; d) S. D. Bergman, F. Wudl, *J. Mater. Chem.* **2008**, *18*, 4; e) R. J. Wojtecki, M. A. Meador, S. J. Rowan, *Nature Mater.* **2011**, *10*, 14.

[5] a) S. R. White, N. R. Sottos, P. H. Geubelle, J. S. Moore, M. R. Kessler, S. R. Sriram, E. N. Brown, S. Viswanathan, *Nature* **2001**, *409*, 794; b) K. S. Toohey, N. R. Sottos, J. A. Lewis, J. S. Moore, S. R. White, *Nat. Mater.* **2007**, *6*, 581; c) C. J. Hansen, W. Wu, K. S. Toohey, N. R. Sottos, S. R. White, J. A. Lewis, *Adv. Mater.* **2009**, *21*, 4143.

[6] a) X. Chen, M. A. Dam, K. Ono, A. Mal, H. Shen, S. R. Nutt, K. Sheran, F. Wudl, *Science* **2002**, *295*, 1698; b) M. Burnworth, L. Tang, J. R. Kumpfer, A. J. Duncan, F. L. Beyer, G. L. Fiore, S. J. Rowan, C. Weder, *Nature* **2011**, *472*, 334; c) A. B. South, L. A. Lyon, *Angew. Chem. Int. Ed.* **2010**, *49*, 767.

[7] a) B. Ghosh, M. W. Urban, *Science* **2009**, *323*, 1458; b) M. M. Caruso, B. J. Blaiszik, S. R. White, N. R. Sottos, J. S. Moore, *Adv. Funct. Mater.* **2008**, *18*, 1898; c) P. Zheng, T. J. McCarthy, *J. Am. Chem. Soc.* **2012**, *134*, 2024; d) J. Fox, J. J. Wie, B. W. Greenland, S. Burattini, W. Hayes, H. M. Colquhoun, M. E. Mackay, S. J. Rowan, *J. Am. Chem. Soc.* **2012**, *134*, 5362; e) Y. Chen, A. M. Kushner, G. A. Williams, Z. Guan, *Nat. Chem.* **2012**, *4*, 467.

[8] a) Z. Zheng, X. Huang, M. Schenderlein, D. Borisova, R. Cao, H. Möhwald, D. Shchukin, *Adv. Funct. Mater.* **2013**, DOI: 10.1002/adfm.201203180; b) M. L. Zheludkevich, D. G. Shchukin, K. A. Yasakau, H. Möhwald, M. G. S. Ferreira, *Chem. Mater.* **2007**, *19*, 402; c) D. V. Andreeva, D. Fix, H. Möhwald, D. G. Shchukin, *Adv. Mater.* **2008**, *20*, 2789.

[9] a) Y. Li, L. Li, J. Sun, *Angew. Chem. Int. Ed.* **2010**, *49*, 6129; b) X. Wang, X. Liu, F. Zhou, W. Liu, *Chem. Commun.* **2011**, *47*, 2324.

[10] a) T.-S. Wong, S. H. Kang, S. K. Y. Tang, E. J. Smythe, B. D. Hatton, A. Grinthal, J. Aizenberg, *Nature* **2011**, *477*, 443; b) H. Wang, Y. Xue, J. Ding, L. Feng, X. Wang, T. Lin, *Angew. Chem. Int. Ed.* **2011**, *50*, 11433.

[11] a) Y. Li, S. Chen, M. Wu, J. Sun, *Adv. Mater.* **2012**, *24*, 4578; b) K. A. Williams, A. J. Boydston, C. W. Bielawski, *J. R. Soc. Interface* **2007**, *4*, 359; c) S. A. Odom, M. M. Caruso, A. D. Finke, A. M. Prokup, J. A. Ritchey, J. H. Leonard, S. R. White, N. R. Sottos, J. S. Moore, *Adv. Funct. Mater.* **2010**, *20*, 1721; d) B. J. Blaiszik, S. L. B. Kramer, M. E. Grady, D. A. McIlroy, J. S. Moore, N. R. Sottos, S. R. White, *Adv. Mater.* **2012**, *24*, 398; e) S. A. Odom, S. Chayanupatkul, B. J. Blaiszik, O. Zhao, A. C. Jackson, P. V. Braun, N. R. Sottos, S. R. White, J. S. Moore, *Adv. Mater.* **2012**, *24*, 2578; f) B. C-K. Tee, C. Wang, R. Allen, Z. Bao, *Nature Nanotechnol.* **2012**, *7*, 825.

[12] a) A. P. Esser-Kahn, N. R. Sottos, S. R. White, J. S. Moore, *J. Am. Chem. Soc.* **2010**, *132*, 10266; b) Y. C. Yuan, M. Z. Rong, M. Q. Zhang, J. Chen, G. C. Yang, X. M. Li, *Macromolecules* **2008**, *41*, 5197; c) S. H. Cho, S. R. White, P. V. Braun, *Chem. Mater.* **2012**, *24*, 4209; d) S. H. Cho, S. R. White, P.V. Braun, *Adv. Mater.* **2009**, *21*, 645.

[13] V. Amendola, M. Meneghetti, *J. Mater. Chem.* **2012**, *22*, 24501.

[14] A. C. Jackson, J. A. Bartelt, P. V. Braun, *Adv. Funct. Mater.* **2011**, *21*, 4705.

[15] a) K. Imato, M. Nishihara, T. Kanehara, Y. Amamoto, A. Takahara, H. Otsuka, *Angew. Chem. Int. Ed.* **2012**, *51*, 1138; b) A. Vidyasagar,

K. Handore, K. M. Sureshan, *Angew. Chem. Int. Ed.* **2011**, *50*, 8021; c) Y. Amamoto, J. Kamada, H. Otsuka, A. Takahara, K. Matyjaszewski, *Angew. Chem. Int. Ed.* **2011**, *50*, 1660; d) P. Cordier, F. Tournilhac, C. Soulié-Ziakovic, L. Leibler, *Nature* **2008**, *451*, 977; e) H. Zhang, H. Xia, Y. Zhao, *ACS Macro Lett.* **2012**, *1*, 1233.

[16] X. Wang, F. Liu, X. Zheng, J. Sun, *Angew. Chem. Int. Ed.* **2011**, *50*, 11378.

[17] a) G. Decher, *Science* **1997**, *227*, 1232 ; b) F. Caruso, R. A. Caruso, H. Möhwald, *Science* **1998**, *282*, 1111; c) X. Zhang, H. Chen, H. Zhang, *Chem. Commun.* **2007**, 1395; d) P. Podsiadlo, M. Michel, J. Lee, E. Verploegen, N. W. S. Kam, V. Ball, J. Lee, Y. Qi, A. J. Hart, P. T. Hammond, N. A. Kotov, *Nano Lett.* **2008**, *8*, 1762; e) Y. Li, X. Wang, J. Sun, *Chem. Soc. Rev.* **2012**, *41*, 5998.

[18] a) D. M. Guldi, I. Zilbermann, G. Anderson, N. A. Kotov, N. Tagmatarchise, M. Prato, *J. Mater. Chem.* **2005**, *15*, 114; b) D. M. Guldi, G. M. A. Rahman, M. Prato, N. Jux, S. Qin, W. Ford, *Angew. Chem. Int. Ed.* **2005**, *44*, 2015.

[19] a) J.-M. Leväsalmi, T. J. McCarthy, *Macromolecules* **1997**, *30*, 1752; b) M. L. Bruening, D. M. Sullivan, *Chem.—Eur. J.* **2002**, *8*, 3833; c) M.-K. Park, S. Deng, R. C. Advincula, *J. Am. Chem. Soc.* **2004**, *126*, 13723; d) Z. Liu, Y. Yi, J. Gauczinski, H. Xu, M. Schönhoff, X. Zhang, *Langmuir* **2011**, *27*, 11806.

[20] a) J. A. Hiller, J. D. Mendelsohn, M. F. Rubner, *Nat. Mater.* **2002**, *1*, 59; b) L. Zhang, Y. Li, J. Sun, J. Shen, *Langmuir* **2008**, *24*, 10851; c) E.-H. Kang, P. Jin, Y. Yang, J. Sun, J. Shen, *Chem. Commun.* **2006**, 4332; d) R. Liang, S. Xu, D. Yan, W. Shi, R. Tian, H. Yan, M. Wei, D. G. Evans, X. Duan, *Adv. Funct. Mater.* **2012**, *22*, 4940.

[21] a) H. Hwang, P. Joo, M. S. Kang, G. Ahn, J. T. Han, B.-S. Kim, J. H. Cho, *ACS Nano* **2012**, *6*, 2432; b) P. Jia, A. A. Argun, J. Xu, S. Xiong, J. Ma, P. T. Hammond, X. Lu, *Chem. Mater.* **2010**, *22*, 6085.

[22] a) Y. Ma, Y. Zhang, B. Wu, W. Sun, Z. Li, J. Sun, *Angew. Chem. Int. Ed.* **2011**, *50*, 6254; b) A. Zhuk, R. Mirza, S. Sukhishvili, *ACS Nano* **2011**, *5*, 8790; c) D. J. Schmidt, F. Ç. Cebeci, Z. I. Kalcioglu, S. G. Wyman, C. Ortiz, K. J. Van Vliet, P. T. Hammond, *ACS Nano* **2009**, *3*, 2207.

[23] a) C. Picart, P. Lavalle, P. Hubert, F. J. G. Cuisinier, G. Decher, P. Schaaf, J.-C. Voegel, *Langmuir* **2001**, *17*, 7414; b) C. Picart, J. Mutterer, L. Richert, Y. Luo, G. D. Prestwich, P. Schaaf, J.-C. Voegel, P. Lavalle, *Proc. Natl. Acad. Sci. USA* **2002**, *99*, 12531.

[24] a) P. M. Nguyen, N. S. Zacharia, E. Verploegen, P. T. Hammond, *Chem. Mater.* **2007**, *19*, 5524; b) B.-S. Kim, S. W. Park, P. T. Hammond, *ACS Nano* **2008**, *2*, 386.

[25] a) A. J. Chung, M. F. Rubner, *Langmuir* **2002**, *18*, 1176; b) J. F. Quinn, F. Caruso, *Langmuir* **2004**, *20*, 20; c) S. E. Burke, C. J. Barrett, *Macromolecules* **2004**, *37*, 5375; d) X. Wang, L. Zhang, L. Wang, J. Sun, J. Shen, *Langmuir* **2010**, *26*, 8187.

[26] a) A. W. Bauer, W. M. M. Kirby, J. C. Sherris, M. Turck, *Am. J. Clin. Pathol.* **1966**, *45*, 493; b) S. Yin, Y. Goldovsky, M. Herzberg, L. Liu, H. Sun, Y. Zhang, F. Meng, X. Cao, D. D. Sun, H. Chen, A. Kushmaro, X. Chen *Adv. Funct. Mater.* **2013**, *23*, 2972.

[27] C. W. Levy, A. Roujeinikova, S. Sedelnikova, P. J. Baker, A. R. Stuitje, A. R. Slabas, D. W. Rice, J. B. Rafferty, *Nature* **1999**, *398*, 383.

[28] a) W. C. Oliver, G. M. Pharr, *J. Mater. Res.* **1992**, *7*, 1564; b) E. G. Herbert, W. C. Oliver, G. M. Pharr, *J. Phys. D: Appl. Phys.* **2008**, *41*, 074021.

[29] J. Wang, F. G. Shi, T. G. Nieh, B. Zhao, M. R. Brongo, S. Qu, T. Rosenmayer, *Scripta Mater.* **2000**, *42*, 687.